Mimicking the Mn_4CaO_5-Cluster in Photosystem II

Yang Chen, Ruoqing Yao, Yanxi Li, Boran Xu, Changhui Chen, and Chunxi Zhang

Abstract The oxygen-evolving center (OEC) in photosystem II (PSII) is a unique biocatalyst that splits water into electrons, protons, and dioxygen. Recent crystallographic studies of PSII have revealed that the structure of the OEC is an asymmetric Mn_4CaO_5-cluster, while the detailed mechanism for the O=O bond formation is still elusive mainly due to the complexity of the large protein environment and structural uncertainty of the OEC during the catalytic reaction. To understand the structure-function relationship and the catalytic mechanism of this natural Mn_4CaO_5-cluster, as well as to develop efficient man-made water-splitting catalysts in artificial photosynthesis, precise mimics of the OEC are highly required. It is of a great challenge to precisely mimic the structure and function of the OEC in the laboratory. However significant advances have recently been achieved. One of the most important advances is the synthesis of a series of the artificial Mn_4CaO_4-clusters that closely mimics both the geometric and electronic structures of the OEC, which provides a structurally well-defined chemical model to investigate the structure-function relationship of the natural Mn_4CaO_5-cluster, and sheds new insights into the mechanism of the water-splitting reaction in PSII. The artificial Mn_4CaO_4-cluster and its variants may open new avenues to develop efficient artificial catalysts for the water-splitting reaction by using earth-abundant and nontoxic chemical elements in the future.

Keywords Photosystem II · Oxygen-evolving center · Mn_4Ca-cluster · Water-splitting reaction · Artificial photosynthesis

Y. Chen · R. Yao · Y. Li · B. Xu
Laboratory of Photochemistry, Institute of Chemistry, Chinese Academy of Sciences, Beijing, China

University of Chinese Academy of Sciences, Beijing, China

C. Chen · C. Zhang (✉)
Laboratory of Photochemistry, Institute of Chemistry, Chinese Academy of Sciences, Beijing, China
e-mail: chunxizhang@iccas.ac.cn

Q. Wang (ed.), *Microbial Photosynthesis*,
https://doi.org/10.1007/978-981-15-3110-1_13

1 Introduction

Photosynthetic oxygen evolution is a unique function of the photosystem II (PSII), which is a pigment-binding, multi-subunit protein complex embedded in the thylakoid membranes of plants, algae, and cyanobacteria (Barber 2009; Dau and Zaharieva 2009; Junge 2019; Lubitz et al. 2019; Nelson and Yocum 2006; Satoh and Wydrzynski 2005; Shen 2015). The reaction center and the key cofactors of PSII involved to perform this function are shown in Fig. 1. Upon photoexcitation, the primary electron donor (P_{680}) donates one electron to the primary electron acceptor (Pheo), producing the $P_{680}^{+\bullet}$ and $Pheo^{-\bullet}$ charge pair in a few picoseconds (Cardona et al. 2012; Diner and Rappaport 2002; Holzwarth et al. 2006; Renger 2012). $Pheo^{-\bullet}$ then transfers the electron to the primary and secondary plastoquinones (Q_A and Q_B) in sequence through the non-heme iron at the acceptor side (Petrouleas and Crofts 2005; Saito et al. 2013). The high redox potential of $P_{680}^{+\bullet}$ obtains one electron from the secondary electron donor (Tyr_Z), leading to the formation of a neutral radical ($Tyr_Z^{\bullet}$) (Diner and Britt 2005; Styring et al. 2012; Zhang 2007), which then drives the water oxidation at the oxygen-evolving center (OEC), in milliseconds at the donor side (Lubitz et al. 2019; McEvoy and Brudvig 2006; Perez-Navarro et al. 2016; Yano and Yachandra 2014).

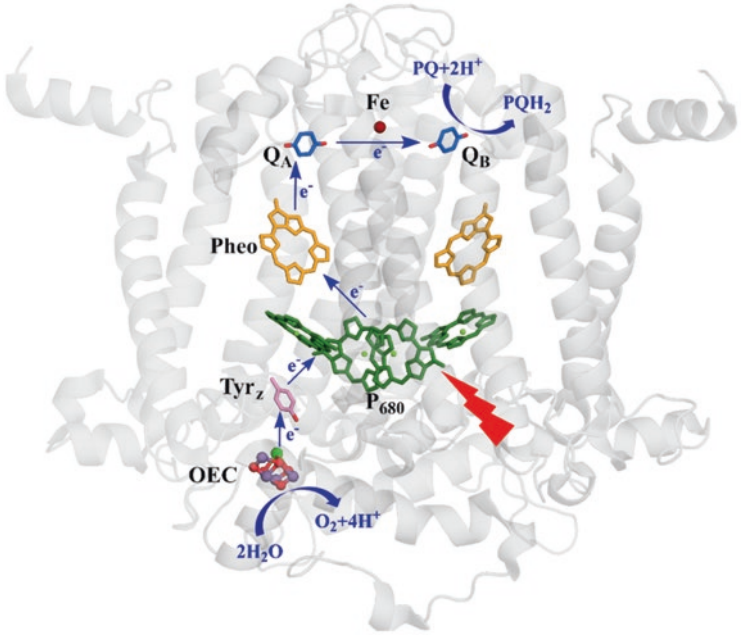

Fig. 1 The reaction center and main cofactors involved for electron transfers and catalytic reactions in PSII (Umena et al. 2011)

The catalytic oxygen-evolving reaction involves five different redox states (S_n, n = 0–4) of the OEC as shown in Fig. 2 (Dau and Haumann 2007; Kok et al. 1970), wherein the S_0 state is the initial and most reduced state and the S_1 state is the dark-stable state. The S_2 and S_3 states are metastable and decay eventually to the dark-stable S_1 state, whereas the S_4 state is a transient state that releases dioxygen and decays to the S_0 state. Changes of the oxidation valences of the four manganese ions occur during the turnover. The oxidation valences for the four manganese ions are S_0 (III, III, III, IV) or (II, III, IV, IV), S_1 (III, III, IV, IV), S_2 (III, IV, IV, IV), and S_3 (IV, IV, IV, IV) (Dau et al. 2008; Krewald et al. 2015; Sauer et al. 2008; Yano and Yachandra 2014). The calcium is an indispensable cofactor for the function of the OEC, and its depletion results in the complete loss of the water oxidation capability of PSII, and it can only be functionally replaced by strontium (Koua et al. 2013; van Gorkom and Yocum 2005; Yocum 2008). Due to the broad interests in fundamental research, as well as potential applications in artificial photosynthesis, the structure and catalytic mechanism of the OEC have attracted extensive studies during the last three decades (Junge 2019; Lubitz et al. 2019; Pantazis 2018).

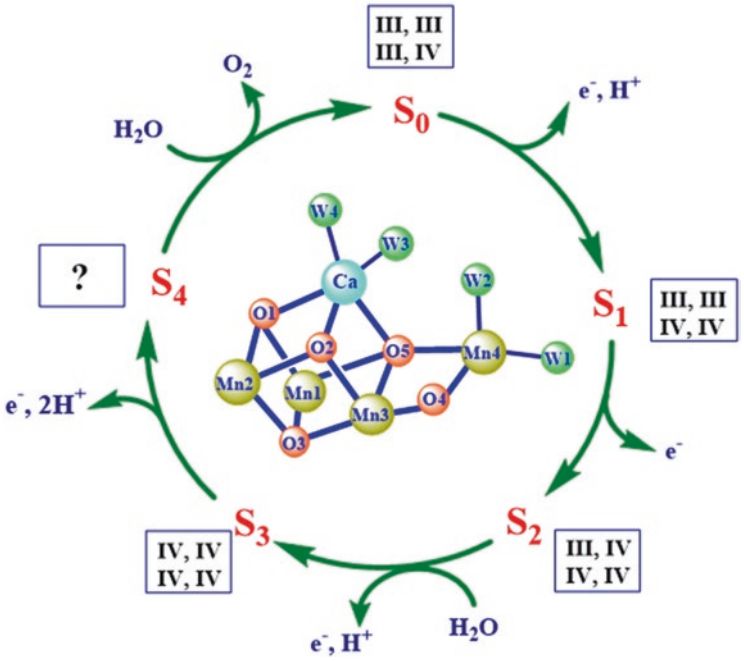

Fig. 2 The turnover of the OEC in PSII (Krewald et al. 2015). The oxidation valences of the four manganese ions in each S state are given in Roman numerals in squares. The structure and the assignment of each atom of the OEC are provided in the middle of this scheme

2 Structure of the OEC

Revealing the structure of the OEC has been a long-standing issue in the field of the photosynthetic research. Before the appearance of the crystal structure of PSII, most structural information of the OEC came from extended X-ray absorption fine structure (EXAFS) (Dau et al. 2008; Yano and Yachandra 2014) and electron paramagnetic resonance (EPR) (Cox et al. 2013; Lubitz et al. 2019; Peloquin and Britt 2001) investigations and theoretical calculations (Siegbahn 2009). Different structural models were proposed to explain the properties of the OEC in PSII (Cinco et al. 1998; Peloquin et al. 2000; Tommos and Babcock 1998; Vrettos et al. 2001). Figure 3a shows the structural model proposed by Zhang et al. in 1999 (Zhang 2016; Zhang et al. 1999), in which the key component of calcium was suggested to be located in the middle of the OEC and be connected with four manganese ions through three oxide bridges and two carboxylate groups. This model was the only model that successfully predicted the binding mode of calcium in OEC of PSII (see below).

The crystal structure data of the PSII have emerged since the beginning of this century (Ferreira et al. 2004; Guskov et al. 2009; Hellmich et al. 2014; Kamiya and Shen 2003; Umena et al. 2011; Zouni et al. 2001). In 2001, Zouni et al. (2001) reported the first crystal structure of PSII from thermophilic cyanobacterium at a resolution of 3.8 Å. In 2004, based on the 3.5 Å resolution structure data, Ferreira et al. (2004), for the first time, proposed that the OEC could be comprised of a Mn_3CaO_4 cubane attached with a "dangler" Mn ion via one bridging oxide, forming a Mn_4CaO_4-cluster. However, the detailed peripheral ligands of the OEC were still elusive due to the low resolution and the possible reduction induced by X-ray radiation during the crystallographic structural determination (Askerka et al. 2017; Grabolle et al. 2006; Yano et al. 2005, 2006).

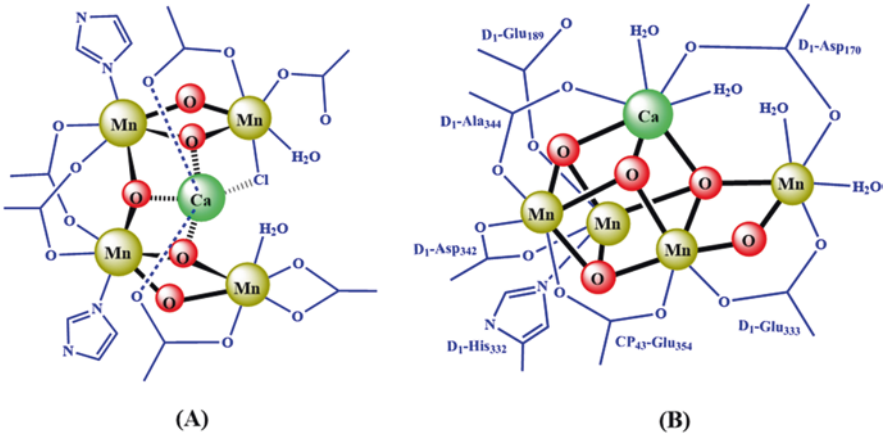

Fig. 3 Scheme for the structural model (Zhang 2016; Zhang et al. 1999) (**a**) and structure (Umena et al. 2011) (**b**) of the OEC

The detailed structure of the OEC was revealed by the crystal structure of PSII at a resolution of 1.9 Å reported by Umena et al. in 2011. All binding ligands of the OEC have been clearly resolved, including four water molecules, one imidazole group from D_1-His332, and six carboxylate groups from D_1-Asp170, D_1-Glu189, D_1-Glu333, D_1-Asp342, D_1-Ala344, and CP_{43}-Glu354, respectively. One additional bridged oxygen (O4) between Mn4 and Mn3 in the OEC has been observed (Fig. 3b). The whole structure of the OEC is an asymmetric Mn_4CaO_5-cluster. In this structure, Ca^{2+} is located in the middle of the OEC and is connected to the Mn_4-cluster through three oxide bridges and two carboxylate groups, which is consistent with our previous proposal (Fig. 3a) published in 1999 (Zhang 2016; Zhang et al. 1999).

The structure of the OEC (Fig. 3b) was further confirmed by the 1.95 Å resolution data obtained by an X-ray free-electron laser (XFEL) reported by Shen's group (Suga et al. 2015, 2017, 2019) and other groups (Kern et al. 2018; Young et al. 2016). It was also supported by the 2.44 Å resolution reported by Hellmich et al. (2014) and 1.87 Å resolution reported by Tanaka et al. by using conventional synchrotron radiation source at extremely low X-ray doses (0.03 MGy) (Tanaka et al. 2017).

Recently, the structure of the OEC in higher plants (spinach and *Pisum sativum*) has also been revealed by single-particle cryoelectron microscopy (cryo-EM) at the resolution of 3.2~2.7 Å (Su et al. 2017; Wei et al. 2016).

The structures of the S_2 and S_3 states OEC were also reported recently by using XFEL. It has been suggested that the structure revealed by XFEL could be corresponding to the native structure of the OEC (Suga et al. 2015). However, consensus of the atomic positions of the S_1 state OEC revealed by XFEL is still not fully reached for all structures with the results of EXAFS spectroscopy studies on active sample (Askerka et al. 2017). To evaluate the oxidation valences of the four manganese ions in the structure of the OEC revealed by XFEL, we have carried out bond-valence sum (BVS) calculations. BVS method is a popular method in coordination chemistry to estimate the oxidation valences of atoms (Brown 2009; Pauling 1929). It is derived from the bond-valence model (Pauling 1929), which is a simple yet robust model for validating chemical structures with localized bonds or used to predict some of their properties. This method has been used extensively to estimate the oxidation state of active site in various metalloenzymes, as well (Gatt et al. 2012; Liu and Thorp 1993). Table 1 lists the results of the BVS calculations on the XFEL's structures of the OEC in the so-called "native" S_1, S_2, and S_3 states, respectively. Surprisingly, the oxidation valences of the four manganese ions of all these states are remarkably lower than that of widely adopted in the field of photosynthetic research (Dau and Haumann 2008; Krewald et al. 2015; Peloquin and Britt 2001; Yano and Yachandra 2014). It is likely that the reduction of the high oxidation valences of manganese ions in the OEC could still take place during the XFEL structural determination. If it was the case, one would expect that the XFEL structures of the OEC would be different from the native structure of these intermediate states during the catalytic cycle. Recently, Amin et al. found that structural modifications of the OEC would take place due to the radiation damage induced by XFEL (Amin et al. 2016); particularly, they found that the position of the μ_4-oxide bridge (O5, Fig. 2) can be significantly disturbed by XFEL.

Table 1 Bond-valence sum (BVS) calculations on the structures of the OEC revealed by X-ray free-electron laser (XFEL) at different resolutions in different S states. Roman numerals in parentheses indicate the assignment of the possible oxidation valences of four manganese ions in the OEC based on BVS calculations. All atomic coordinates were taken from the first monomer of photosystem II in the crystal structure data with PDB-IDs: 4UB6, 6DHF, 6JLK, 6DHO, and 6JLL, respectively

Resolution of PSII	S_1 (1.95 Å) (4UB6)	S_2 (2.08 Å) (6DHF)	S_2 (2.15 Å) (6JLK)	S_3 (2.07 Å) (6DHO)	S_3 (2.15 Å) (6JLL)
Mn1	3.075 (III)	3.232 (III)	3.204 (III)	3.901 (IV)	4.300 (IV)
Mn2	3.237 (III)	4.316 (IV)	3.775 (IV)	4.193 (IV)	3.852 (IV)
Mn3	2.980 (III)	3.784 (IV)	3.347 (III)	3.232 (III)	3.243 (III)
Mn4	2.318 (II)	3.139 (III)	2.597 (III)	2.932 (III)	2.531 (III)

3 Mechanism for the Water-Splitting Reaction in the OEC

Based on recent crystallographic studies (Ferreira et al. 2004; Kern et al. 2018; Suga et al. 2017, 2019; Umena et al. 2011), spectroscopic investigations (Cox et al. 2014), as well as theoretical calculations (Siegbahn 2013; Yamaguchi et al. 2018), different proposals for the O=O bond formation have been suggested. Figures 4, 5, and 6 show three typical models proposed by different groups.

The mechanism in Fig. 4 was suggested by Barber's group, in which the two oxygen of two water molecules (W2 and W3) were proposed to serve as the oxygen sources for the formation of the O=O bond. The key feature of this mechanism is that the O–O bond is formed by a nucleophilic attack of a calcium-ligated hydroxyl group onto an electrophilic oxo of $Mn^{V} \equiv O$ or Mn^{IV}-$O^{\bullet}$, derived from the deprotonation of the second substrate water molecule. Similar proposals have been suggested by other groups (Chen et al. 2015; Vinyard et al. 2015). However, this proposal was not supported by recent theoretical calculation reported by Siegbahn (Siegbahn 2017).

The second proposal for the mechanism of the water-splitting reaction was suggested by Ishikita's group as shown in Fig. 5 (Kawashima et al. 2018). In this mechanism, the μ_2-oxide bridge (O4) and one water molecule (W1) were suggested to provide the oxygen atoms to form the O=O bond. The key feature of this proposal is that the O-O bond could be formed through the coupling of a bridged oxo and an Mn(IV)-$O^{\bullet}$ oxyl radical. However, the oxidation valences (III, IV, IV, IV) of the four manganese ions in the S_3 state were not consistent with the widely accepted values of (IV, IV, IV, IV).

The third mechanism was suggested by Siegbahn based on theoretical calculations (Siegbahn 2013)(Fig. 6). The main feature of this proposal is that the μ_4-oxide bridge (O5) serves as the active site for the O=O bond formation. Some recent crystallographic results (Suga et al. 2019) and spectroscopic studies (Cox et al. 2014) show experimental evidence to support this proposal in some degree; however, it is still an open question whether the Mn1 is the active site for the binding site of the second substrate water molecule. According to this mechanism, remarkably, the release of O_2 from the S_4 state would result in the formation of four unsaturated

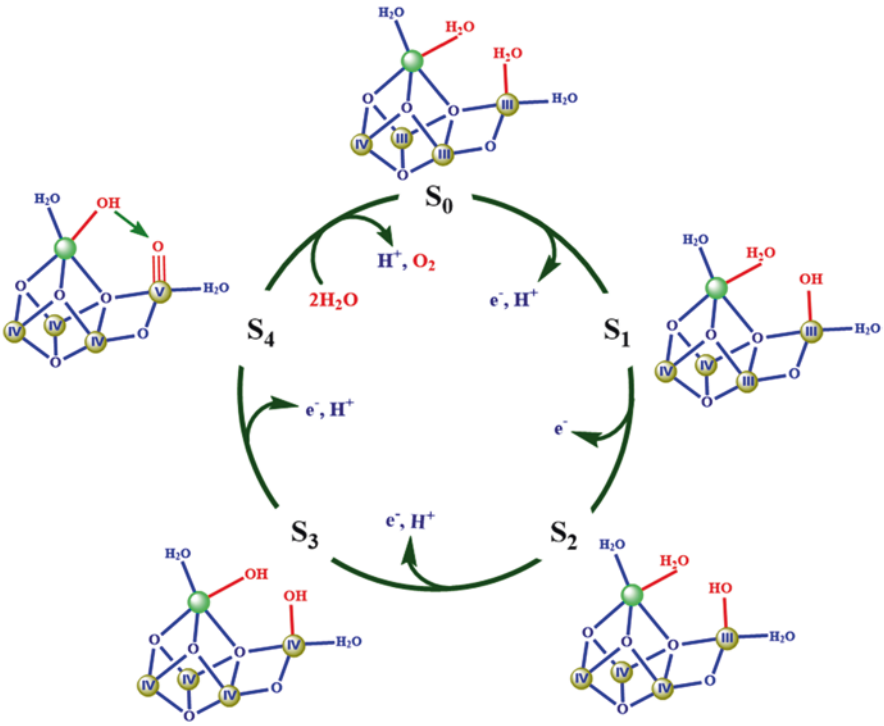

Fig. 4 One possible mechanism for the water-splitting reaction by OEC suggested by Barber's group. Significant changes during the catalytic cycle are given in red color. Mn and Ca are shown in brown and green, respectively. Roman numerals indicate the oxidation states of manganese ions

metal ions, namely, three five-coordinated manganese (i.e., Mn1, Mn3, Mn4) and one six-coordinated calcium (Zhang and Kuang 2018), which could certainly require much high activation energy. Thus, one would expect that the dioxygen release could be the rate-limited step during the catalytic cycle, which is inconsistent with the fast release of the O_2 observed in natural system (Haumann et al. 2005; Junge 2019). It is also noted that the suggestion of the protonated μ_4-oxide bridge (i.e., OH) for O5 has not been supported by the theoretical studies from other group (Ishikita 2019).

As mentioned above, although various mechanisms for the water-splitting reaction have been proposed (Barber 2017; Chen et al. 2015; Isobe et al. 2012; Kawashima et al. 2018; Krewald et al. 2016; Siegbahn 2013; Vinyard et al. 2015), the detailed mechanism for the O=O bond formation is still fully unknown (Junge 2019; Pantazis 2018) due to the complexity of the huge protein environment and the dynamic structural changes of the OEC during the water-splitting reaction. In this regard, therefore, precise structural information for different S states of the OEC is highly required in the future (Kern et al. 2018; Suga et al. 2017, 2019; Young et al. 2016; Zhang and Kuang 2018).

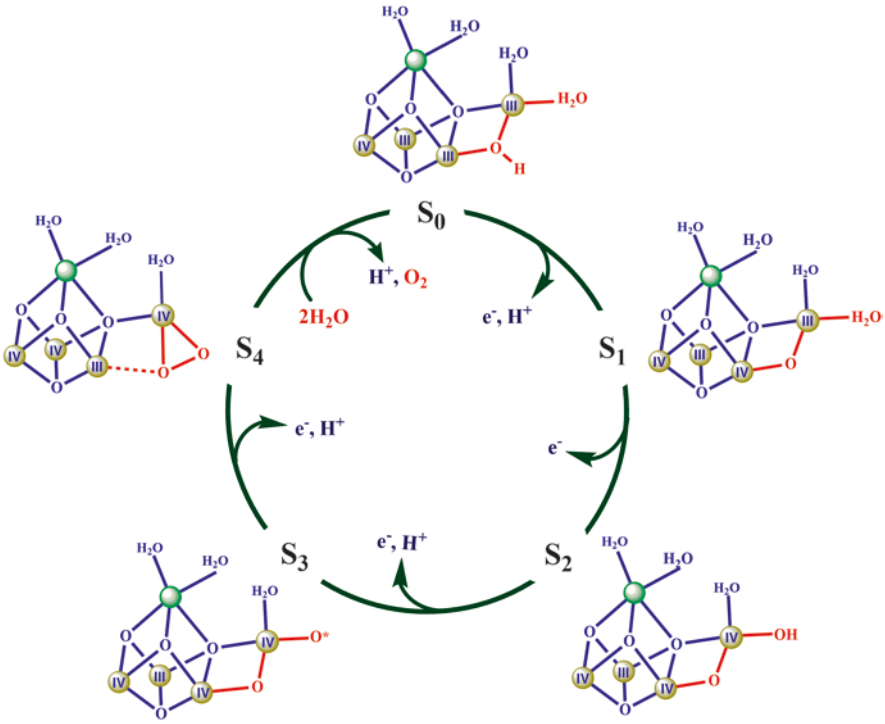

Fig. 5 The second proposal for the O=O bond formation involving the μ_2-oxide bridge (O4) and W1. Significant changes during the catalytic cycle are given in red color. Mn and Ca are shown in brown and green, respectively. Roman numerals indicate the oxidation states of manganese ions

4 Challenge for the Synthesis of the OEC in Laboratory

In order to better understand the structure and properties of the OEC, as well as to develop highly efficient and cheap artificial catalysts for the water-splitting reaction to overcome the bottleneck of artificial photosynthesis, many groups have tried to synthesize the OEC in laboratory since the end of last century. However, it was a great challenge for chemists to synthesize the entire structure of the OEC in laboratory due to several reasons (Zhang 2015, 2016): (1) It is very difficult to incorporate Ca^{2+} into the Mn_4-cluster through μ-oxo bridges, because the affinity of Ca^{2+} to μ-oxo is significantly weaker than that of Mn ion. In general, only a multi-manganese cluster, instead of the manganese-calcium heterometallic cluster, can be synthesized. (2) The core structure of the OEC is an asymmetric Mn_4Ca-cluster. It was unknown whether such a structure could be synthesized in a chemical system. (3) The ligands of the biological OEC are mainly composed of carboxylate groups and water molecules, which are drastically different from the multi-pyridine ligands used in most previous chemical model systems (Kärkäs et al. 2014; Limburg et al. 1999; Mullins and Pecoraro 2008; Tsui et al. 2013). (iv) The redox potential of the

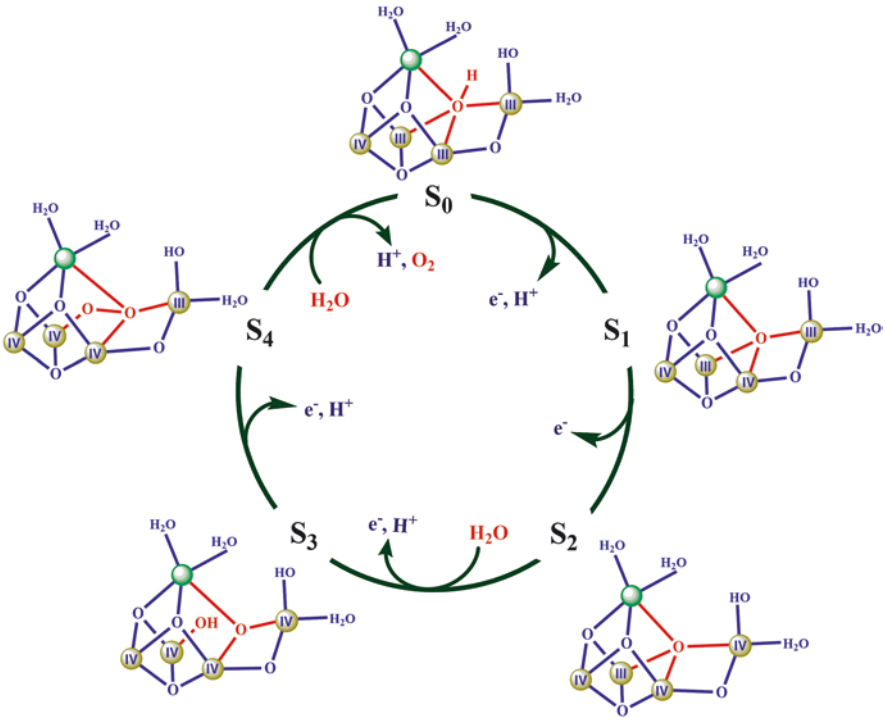

Fig. 6 The third proposal for the O=O bond formation involved the μ_4-oxide bridge (O5). Significant changes during the catalytic cycle are given in red color. Mn and Ca are shown in brown and green, respectively. Roman numerals indicate the oxidation states of manganese ions

OEC is very high (+0.8 ~ +1.0 V vs. NHE) (Dau and Zaharieva 2009; Vass and Styring 1991) due to the presence of the high oxidation states of the manganese ions.

A large number of artificial Mn complexes have been reported in the literature (Dismukes et al. 2009; Gerey et al. 2016; Limburg et al. 1999; Mukhopadhyay et al. 2004; Mullins and Pecoraro 2008; Najafpour et al. 2016; Paul et al. 2017). Among them, tetra-manganese complexes containing Mn_4O_4-cubane (Chakov et al. 2003, 2016; Dismukes et al. 2009; Kanady et al. 2011; Ruettinger et al. 1997) (Fig. 7) are attractive, because the oxidation states of the four manganese ions are (III, III, IV, IV) similar to that of the OEC in the S_1 state (Fig. 2). The peripheral ligands in these artificial complexes, however, it is remarkably different to that of the OEC composing mainly of carboxylate groups (Umena et al. 2011).

Significant advances for the synthesis of the OEC have emerged since 2011. Agapie's group reported the first artificial Mn_3CaO_4-cluster using a multi-pyridylalkoxide ligand (Fig. 8a, b) (Kanady et al. 2011). The same group reported a series of analogues or derivatives (Tsui and Agapie 2013), for example, the artificial Mn_3CaAgO_4-complex (Kanady et al. 2014) (Fig. 8e, f). In 2012, Christou's group reported the $Mn_3Ca_2O_4$-complex with one Ca^{2+} attached to the Mn_3CaO_4 cubane (Mukherjee et al. 2012) (Fig. 8c, d). Distinct from previous Mn_3CaO_4-complexes,

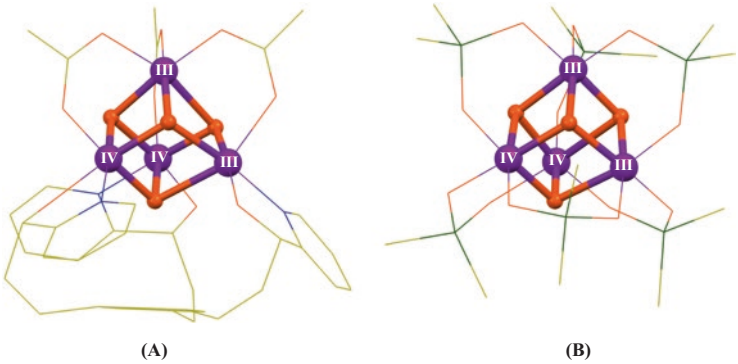

Fig. 7 Structures of two artificial clusters containing Mn_4O_4-cubane. (**a**) $Mn_4O_4L(CH_3CO_2)_3$ complex (L = 1,3,5-tris(2-di(2′-pyridyl)oxymethylphenyl)benzene) (Kanady et al. 2011); (**b**) $Mn_4O_4[(CH_3)_2AsO_2]_6$ complex (Chakov et al. 2016). Mn, O, N, As, and C are shown in purple, orange, blue, dark green, and yellow, respectively. For clarity, all the hydrogen atoms are not shown. Distances are given in Å

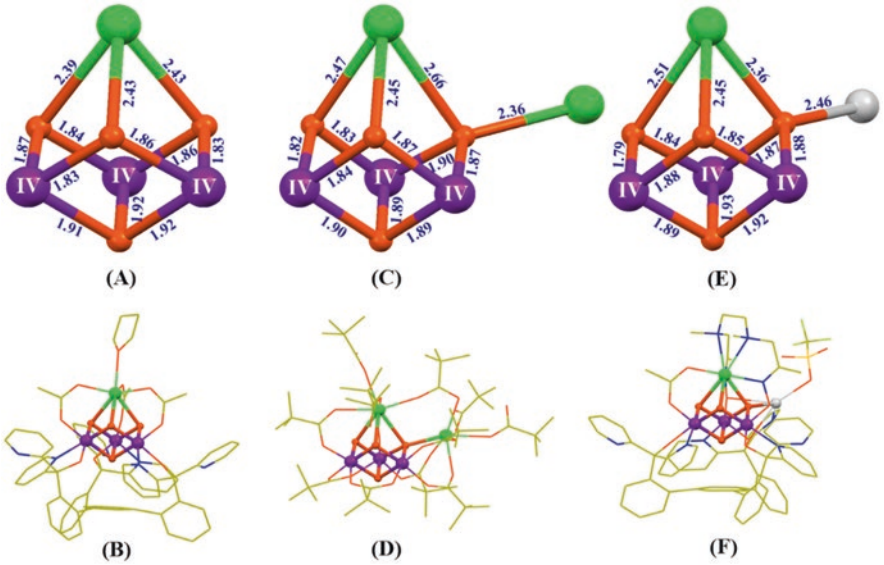

Fig. 8 Structures of artificial complexes containing Mn_3CaO_4 cubane. (**a**) Core structure of the Mn_3CaO_4-complex; (**b**) whole structure of the Mn_3CaO_4-complex (Kanady et al. 2011); (**c**) core structure of the $Mn_3Ca_2O_4$-complex; (**d**) whole structure of the $Mn_3Ca_2O_4$-complex (Mukherjee et al. 2012); (**e**) core structure of the Mn_3CaAgO_4-complex; (**f**) whole structure of the Mn_3CaAgO_4-complex (Kanady et al. 2014). Distances are given in Å units; Mn, Ca, Ag, O, N, F, S, and C are shown in purple, green, gray, orange, blue, green yellow, bright yellow, and yellow, respectively. For clarity, all hydrogen atoms are not shown

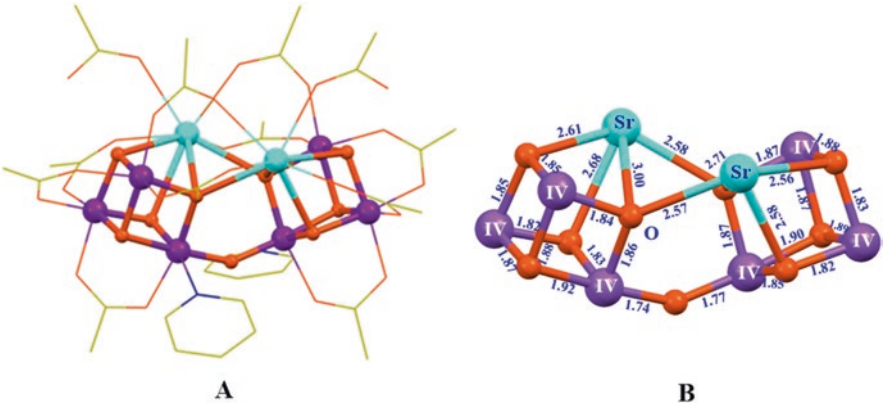

Fig. 9 Structure of the $Mn_6Sr_2O_9$-complex (Chen et al. 2014). (**a**) Whole structure of the $Mn_6Sr_2O_9$-complex; (**b**) core structure of the $Mn_6Sr_2O_9$-complex; Mn, Sr, O, N, and C are shown in purple, cyan, orange, blue, and yellow, respectively. For clarity, all the methyl groups and all the hydrogen atoms are not shown

the peripheral ligands of the $Mn_3Ca_2O_4$-complex are pivalic anions or neutral pivalic acid, closely mimicking the peripheral carboxylate ligands of the OEC in PSII. In these artificial complexes, all the manganese ions are in IV oxidation state, and the typical bond lengths for Mn-O and Ca-O are in the range of 1.8–1.9 Å and 2.4–2.7 Å, respectively. The distances of the Mn…Mn and Mn…Ca are in the range of 2.7–2.8 Å and 3.2–3.5 Å, respectively. In 2014, Zhang's group reported a heterometallic cluster containing two $Mn^{IV}{}_3SrO_4$-cluster linked by one μ_2-oxide bridge (Chen et al. 2014), which mimics the three types of oxide bridges (μ_2-oxide, μ_3-oxide, and μ_4-oxide) and the Mn_3SrO_4 cubane of the Sr^{2+}-containing OEC (Koua et al. 2013) at the same time.

It should be pointed out that although all complexes shown in Figs. 7, 8, and 9 have mimicked some key structural motifs of the Mn_3CaO_4 or Mn_3SrO_4 cubane in the OEC, until recently, it remains a great challenge to synthesize the entire Mn_4Ca-cluster with similar ligands as seen in the OEC of PSII.

5 Closer Mimicking of the OEC

Inspired by the assembly processes of the OEC in PSII (Dasgupta et al. 2008; Zhang et al. 2017), we successfully prepared the first artificial Mn_4Ca-cluster (Zhang et al. 2015) (Fig. 10b, d). It was synthesized through a two-step procedure using inexpensive commercial chemicals. The first step was to synthesize a precursor through a reaction of $Bu^n{}_4NMnO_4$ (Bu^n = n-butyl), $Mn(CH_3CO_2)_2{\bullet}(H_2O)_4$, and $Ca(CH_3CO_2)_2{\bullet}H_2O$ (molar ratio of 4:1:1) in boiling acetonitrile in the presence of an excess of pivalic acid. The second step was to treat the precursor with organic base (pyridine) in ethyl acetate, leading to the formation of final product.

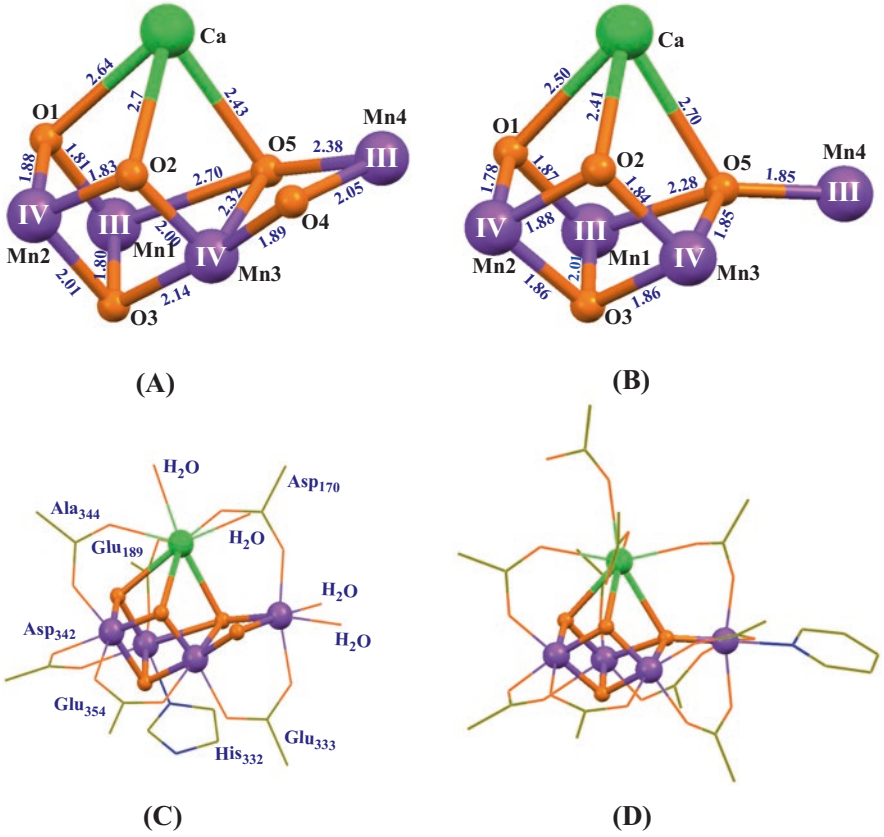

Fig. 10 Structures of the natural OEC (Suga et al. 2015) (**a**, **c**) and the artificial Mn_4Ca-cluster (Zhang et al. 2015) (**b**, **d**). Distances are given in Å units; Mn, Ca, O, N, and C are shown in purple, green, orange, blue, and yellow, respectively. For clarity, all hydrogen atoms are not shown

The core structure of the artificial Mn_4CaO_4-complex contains a Mn_3CaO_4 cubane attached with a dangler Mn ion forming an asymmetric Mn_4CaO_4-cluster, which is exactly the same as the OEC's structure proposed by Ferreira et al. in 2004. The surrounding ligands of the Mn_4CaO_4-cluster are provided by eight $(CH_3)_3CCO_2^-$ anions and three exchangeable neutral ligands (two pivalic acid and one pyridine molecules), similar to the peripheral ligands of the OEC (Fig. 10c).

It should be pointed out that the structure of the artificial Mn_4CaO_4-cluster is well-defined and effect from the X-ray radiation reduction is limited mainly due to the absence of water as solvent in the crystal of the artificial Mn_4CaO_4-complex. BVS calculations have clearly shown that the oxidation states of the four manganese ions of the artificial Mn_4CaO_4-complex are (III, III, IV, IV), which are essentially the same as that proposal for the S_1 state (Fig. 2).

The similarity between the artificial Mn_4CaO_4-cluster and OEC was further supported by the observation of four redox transitions revealed by cyclic voltammo-

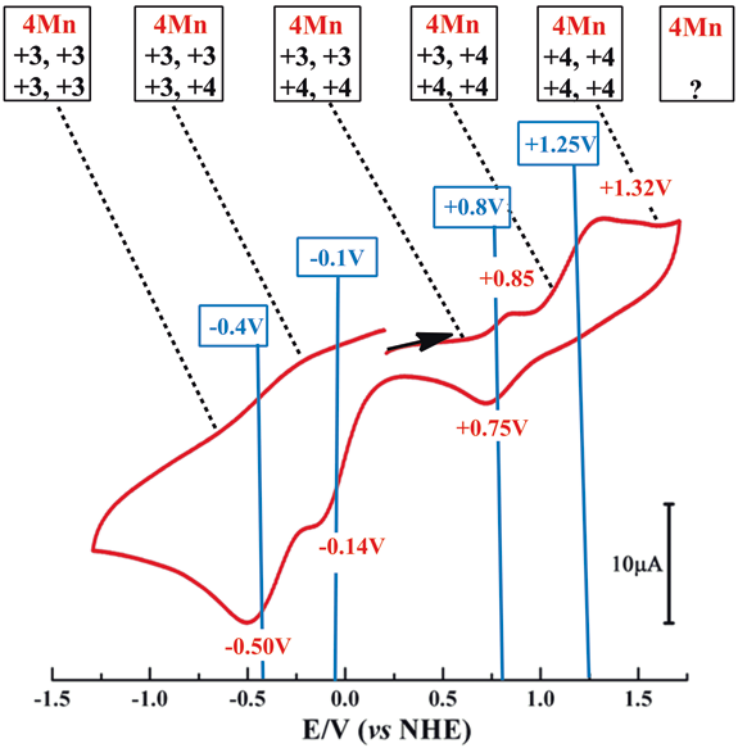

Fig. 11 Cyclic voltammogram (CV) of artificial Mn_4CaO_4-complex in Fig. 10 (Zhang et al. 2015). Potentials vs. NHE; scan rate of 100 mV/s. Peak positions of CV waves are in red and estimated midpoint potentials are in blue. The likely oxidation states of the four Mn ions in various oxidation states of artificial complex are indicated using black numbers

gram (CV) measurements (Fig. 11). The redox potential of ~ 0.8 eV (vs. NHE) for the $S_1 \rightarrow S_2$ transition of artificial Mn_4CaO_4-complex is close to the estimated potential of the corresponding OEC redox transition (≥0.9 V) (Dau and Zaharieva 2009; Vass and Styring 1991) but is remarkably different from that of the previously Mn_3CaO_4-complex without a dangling Mn ion (Kanady et al. 2011). This result indicates that the dangler manganese ion could play a crucial role in tuning the redox potential of Mn_4CaO_4-cluster.

Moreover, the one-electron oxidation of the artificial Mn_4Ca-complex gave rise to two distinct EPR signals ($g = 4.9$ and $g = 2.0$) (Zhang et al. 2015) (Fig. 12a), similar to the $g \approx 4$ and $g = 2.0$ EPR signals (Fig. 12b) observed in PSII for the OEC in the S_2 state (Boussac and Rutherford 2000; Boussac et al. 2018; Dismukes and Siderer 1981; Pantazis et al. 2012; Peloquin and Britt 2001). In the field of photosynthetic research, the latter two EPR signals have been considered as fingerprint spectroscopic characteristics to evaluate the structure and function of the OEC. Therefore, the experimental observation of two EPR signals strongly suggested that the artificial Mn_4Ca-cluster could have similar electronic structures as that of the OEC.

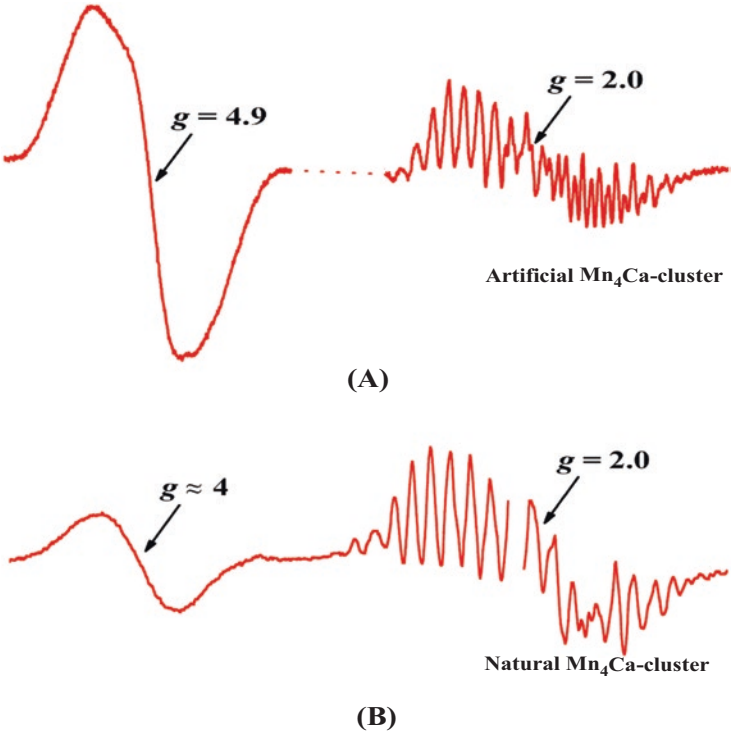

Fig. 12 EPR signals induced from the one-electron oxidation of the artificial Mn_4CaO_4-cluster (Zhang et al. 2015) (**a**) and the OEC in S_2 states (Peloquin and Britt 2001) (**b**). Catalytic activity of the artificial Mn4CaO4-cluster

Considering the close mimicking of both the atomic and electronic structures as well as the redox properties of the OEC, we expect that the artificial Mn_4CaO_4-cluster should be able to serve as a catalyst for the water-splitting reaction. Indeed, a remarkable catalytic current was observed during the CV measurement in the presence of artificial Mn_4CaO_4-complex and 1% water in acetonitrile (Zhang et al. 2015) (Fig. 13a). The artificial Mn_4CaO_4-complexes can also catalyze oxygen-evolving reaction efficiently by using $(CH_3)_3COOH$ (tert-butyl hydroperoxide) as an oxidant in acetonitrile with the presence of 4.5% water (Chen et al. 2017) (Fig. 13b). However, these artificial complexes are very sensitive to the experimental conditions. Quantification of the catalytic reaction has been difficult due to the rapid degradation of the catalyst in the presence of water in solution, making it difficult to quantify the catalytic reaction. The calcium in the artificial complex has been found to be easily dissociated, leading to the formation of multi-manganese complexes.

To improve the stability of the artificial Mn_4CaO_4-cluster, recently, we have prepared two new Mn_4CaO_4-clusters with exchangeable solvent, acetonitrile and N,N-dimethylformamide (DMF) (Chen et al. 2019), on the calcium as shown in Fig. 14. Remarkably, the replacement of one or two ligands on the calcium by organic sol-

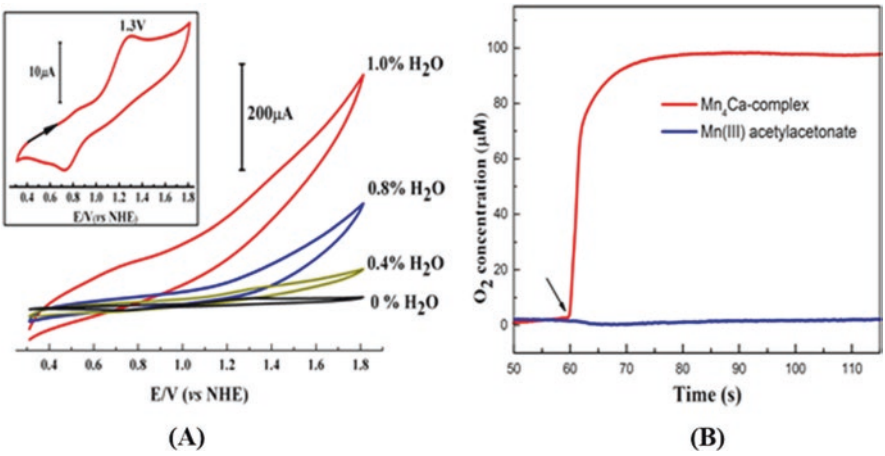

Fig. 13 Catalytic properties of the artificial Mn_4CaO_4-cluster. (**a**) CV measurement of artificial Mn_4CaO_4-complex in acetonitrile with different amounts of H_2O (Zhang et al. 2015). The inset shows the CV without H_2O (0% H_2O). Potentials are referenced to NHE; scan rate, 100 mV/s. (**b**) Oxygen-evolving reaction catalyzed by artificial Mn_4Ca-complex (50 μM) in acetonitrile with the presence of $(CH_3)_3COOH$ (1 M) and 4.5% water in acetonitrile at 25 °C (Chen et al. 2017). A Clark-type O_2 electrode was used to detect the release of dioxygen

vent molecules does not modify the core structure and oxidation valences of the four manganese ions, as well as main peripheral environment ligands. More importantly, these new Mn_4CaO_4-clusters become much stable in the polar solvent, which may provide great opportunity to investigate the catalytic activity of the artificial Mn_4CaO_4-cluster in the future.

6 Implications for the Mechanism of the Water-Splitting Reaction in OEC

Artificial Mn_4CaO_4-clusters shown in Figs. 10 and 14 have mimicked the main structural motifs of the OEC, which could provide distinct structural insight into understanding the principle of the OEC. Firstly, the successful isolation of different artificial Mn_4CaO_4-complexes demonstrates that the Mn_4CaO_4-cluster is thermodynamically stable, supporting the proposal that the Mn_4CaO_4-cluster could be an evolutionary origin of the natural OEC by Barber previously (Barber 2016). Secondly, from the structure of artificial Mn_4CaO_4-cluster, one can clearly see that the μ_4-O^{2-} bridge (O5) is tightly bound to four metal ions (one calcium and three manganese ions). This is a position less prone to be removed or replaced, indicating that the similar μ_4-O^{2-} bridge (O5) in OEC could not be directly involved in serving as an oxygen source to form the O-O bond. Interestingly, Kawashima et al. recently have proposed that the μ_2-O^{2-} bridge (O4) in OEC (Fig. 5), instead, may play a role as the

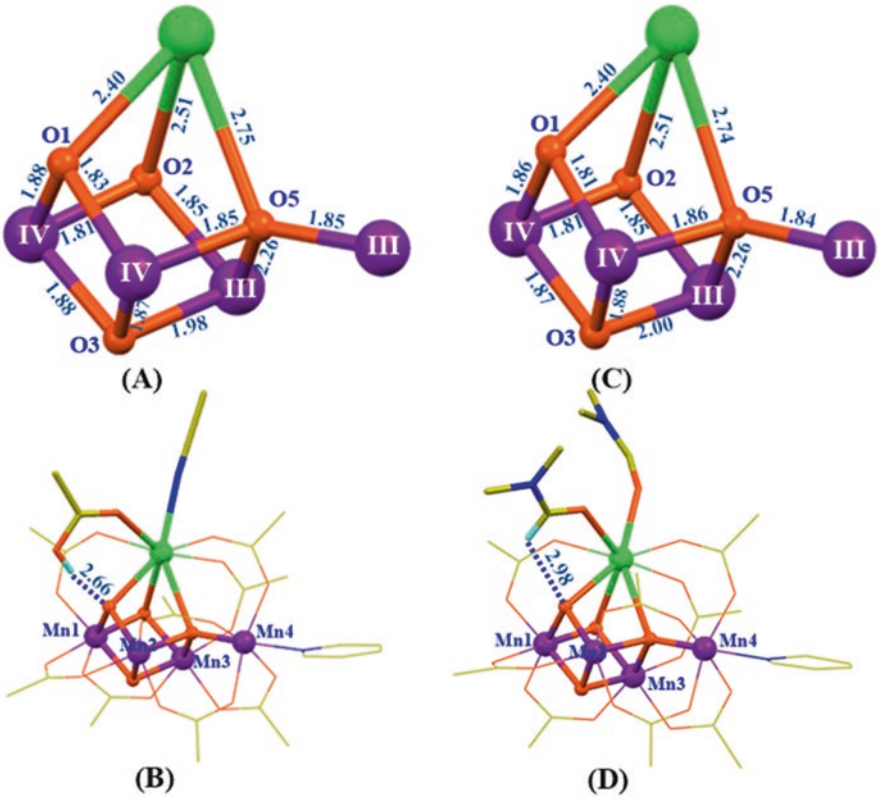

Fig. 14 Crystal structures of two new artificial Mn_4CaO_4-complexes with exchangeable solvent, acetonitrile (**a**, **b**) and N,N-dimethylformamide (**c**, **d**) on the calcium (Chen et al. 2019). Dashed lines indicate the hydrogen bonds. Mn, Ca, O, N, C, and H are shown in purple, green, orange, blue, yellow, and cyan, respectively. Distances are given in Å. The oxidation states of four manganese ions are obtained by the BVS calculation. For clarity, all the methyl groups of pivalic acid are omitted, and only the H atoms involved to form hydrogen bonds are shown

substrate binding site to form the O-O bond (Kawashima et al. 2018). In this proposal and some previous suggestions (Barber 2017; Chen et al. 2015; Vinyard et al. 2015), the Mn_4CaO_4 fragment does not undertake significant changes during the water-splitting reaction, which is consistent with the isolation of the stable artificial Mn_4CaO_4-cluster described here. It should be pointed out that the μ_2-O^{2-} (O4) in OEC is absent in the artificial Mn_4CaO_4-cluster, which is replaced by a bridging carboxyl group in the latter. Obviously, the further investigation of this missing μ_2-O^{2-} bridge in artificial Mn_4Ca-cluster would provide new insights into the mechanism for the O-O bond formation during the OEC turnover.

7 Conclusion

Although the crystallographic studies of PSII have revealed the structure of the OEC, the detailed mechanism for the water-splitting reaction is still elusive due to the complexity of the large protein environment and structural uncertainty of the intermediate states of the OEC during its turnover. To understand the structure-function relationship and the catalytic mechanism of this natural Mn_4CaO_5-cluster, as well as to develop efficient man-made water-splitting catalysts in artificial photosynthesis, many artificial complexes have been synthesized to mimic the OEC in the laboratory. One of the most important advances is the synthesis of a series of the artificial Mn_4CaO_4-clusters that closely mimics both geometric and electronic structures of the OEC, which provides a structurally well-defined chemical model to investigate the structure-function relationship of the natural Mn_4CaO_5-cluster, and sheds new insights into the mechanism of the water-splitting reaction in PSII. This new advance may open new avenues to develop efficient artificial catalysts for the water-splitting reaction by using earth-abundant and nontoxic chemical elements in the future.

Acknowledgment This work was supported by the National Key Research and Development Program of China (No. 2017YFA0503704), the Strategic Priority Research Program of Chinese Academy of Sciences (No. XDA21010212; XDB17030600), and National Natural Science Foundation of China (No. 31770258).

References

Amin, M., Badawi, A., & Obayya, S. S. (2016). Radiation damage in XFEL: Case study from the oxygen-evolving complex of photosystem II. *Scientific Reports, 6*, 36492.

Askerka, M., Brudvig, G. W., & Batista, V. S. (2017). The O_2-evolving complex of photosystem II: Recent insights from quantum mechanics/molecular mechanics (QM/MM), extended X-ray absorption fine structure (EXAFS), and femtosecond X-ray crystallography data. *Accounts of Chemical Research, 50*, 41–48.

Barber, J. (2009). Photosynthetic energy conversion: Natural and artificial. *Chemical Society Reviews, 38*, 185–196.

Barber, J. (2016). Mn_4Ca cluster of photosynthetic oxygen-evolving center: Structure, function and evolution. *Biochemistry, 55*, 5901–5906.

Barber, J. (2017). A mechanism for water splitting and oxygen production in photosynthesis. *Nature Plants, 3*, 17041.

Boussac, A., & Rutherford, A. W. (2000). Comparative study of the g=4.1 EPR signals in the S_2 state of photosystem II. *Biochimica et Biophysica Acta, 1457*, 145–156.

Boussac, A., Ugur, I., Marion, A., Sugiura, M., Kaila, V. R. I., & Rutherford, A. W. (2018). The low spin-high spin equilibrium in the S_2-state of the water oxidizing enzyme. *Biochimica et Biophysica Acta, 1859*, 342–356.

Brown, I. D. (2009). Recent developments in the methods and applications of the bond valence model. *Chemical Reviews, 109*, 6858–6919.

Cardona, T., Sedoud, A., Cox, N., & Rutherford, A. W. (2012). Charge separation in photosystem II: A comparative and evolutionary overview. *Biochimica et Biophysica Acta, 1817*, 26–43.

Chakov, N. E., Abboud, K. A., Zakharov, L. N., Rheingold, A. L., Hendrickson, D. N., & Christou, G. (2003). Reaction of $[Mn_{12}O_{12}(O_2CR)_{16}(H_2O)_4]$ single-molecule magnets with non-carboxylate ligands. *Polyhedron, 22*, 1759–1763.

Chakov, N. E., Thuijs, A. E., Wernsdorfer, W., Rheingold, A. L., Abboud, K. A., & Christou, G. (2016). Unusual $Mn(III/IV)_4$ cubane and $Mn(III)_{16}M_4$ (M = Ca, Sr) looplike clusters from the use of dimethylarsinic acid. *Inorganic Chemistry, 55*, 8468–8477.

Chen, C., Zhang, C., Dong, H., & Zhao, J. (2014). A synthetic model for the oxygen-evolving complex in Sr^{2+}-containing photosystem II. *Chemical Communications, 50*, 9263–9265.

Chen, C., Zhang, C., Dong, H., & Zhao, J. (2015). Artificial synthetic $Mn^{IV}Ca$-oxido complexes mimic the oxygen-evolving complex in photosystem II. *Dalton Transactions, 44*, 4431–4435.

Chen, C., Li, Y., Zhao, G., Yao, R., & Zhang, C. (2017). Natural and artificial Mn_4Ca cluster for the water splitting reaction. *ChemSusChem, 10*, 4403–4408.

Chen, C., Chen, Y., Yao, R., Li, Y., & Zhang, C. (2019). Artificial Mn_4Ca clusters with exchangeable solvent molecules mimicking the oxygen-evolving center in photosynthesis. *Angewandte Chemie, International Edition, 58*, 3939–3942.

Cinco, R. M., Robblee, J. H., Rompel, A., Fernandez, C., Yachandra, V. K., Sauer, K., & Klein, M. P. (1998). Strontium EXAFS reveals the proximity of calcium to the manganese cluster of oxygen-evolving photosystem II. *The Journal of Physical Chemistry. B, 102*, 8248–8256.

Cox, N., Pantazis, D. A., Neese, F., & Lubitz, W. (2013). Biological water oxidation. *Accounts of Chemical Research, 46*, 1588–1596.

Cox, N., Retegan, M., Neese, F., Pantazis, D. A., Boussac, A., & Lubitz, W. (2014). Electronic structure of the oxygen-evolving complex in photosystem II prior to O-O bond formation. *Science, 345*, 804–808.

Dasgupta, J., Ananyev, G. M., & Dismukes, G. C. (2008). Photoassembly of the water-oxidizing complex in photosystem II. *Coordination Chemistry Reviews, 252*, 347–360.

Dau, H., & Haumann, M. (2007). Eight steps preceding O–O bond formation in oxygenic photosynthesis—A basic reaction cycle of the photosystem II manganese complex. *Biochimica et Biophysica Acta, 1767*, 472–483.

Dau, H., & Haumann, M. (2008). The manganese complex of photosystem II in its reaction cycle—Basic framework and possible realization at the atomic level. *Coordination Chemistry Reviews, 252*, 273–295.

Dau, H., & Zaharieva, I. (2009). Principles, efficiency and blueprint character of solar-energy conversion in photosynthetic water oxidation. *Accounts of Chemical Research, 42*, 1861–1870.

Dau, H., Grundmeier, A., Loja, P., & Haumann, M. (2008). On the structure of the manganese complex of photosystem II: Extended-range EXAFS data and specific atomic-resolution models for four S-states. *Philosophical Transactions of the Royal Society of London B, 363*, 1237–1244.

Diner, B. A., & Britt, R. D. (2005). The redox-active tyrosines Y_Z and Y_D. In T. J. Wydrzynski & K. Satoh (Eds.), *Photosystem II: The light-driven water: Plastoquinone oxidoreductase* (pp. 207–233). Dordrecht: Springer.

Diner, B. A., & Rappaport, F. (2002). Structure, dynamics, and energetics of the primary photochemistry of photosystem II of oxygenic photosynthesis. *Annual Review of Plant Biology, 53*, 551–580.

Dismukes, G. C., & Siderer, Y. (1981). Intermediates of a polynuclear manganese center involved in photosynthetic oxidation of water. *Proceedings of the National Academy of Sciences of the United States of America, 78*, 274–278.

Dismukes, G. C., Brimblecombe, R., Felton, G. A. N., Pryadun, R. S., Sheats, J. E., Spiccia, L., & Swiegers, G. F. (2009). Development of bioinspired Mn_4O_4-cubane water oxidation catalysts: Lessons from photosynthesis. *Accounts of Chemical Research, 42*, 1935–1943.

Ferreira, K. N., Iverson, T. M., Maghlaoui, K., Barber, J., & Iwata, S. (2004). Architecture of the photosynthetic oxygen-evolving center. *Science, 303*, 1831–1838.

Gatt, P., Petrie, S., Stranger, R., & Pace, R. J. (2012). Rationalizing the 1.9 Å crystal structure of photosystem II—A remarkable Jahn-Teller balancing act induced by a single proton transfer. *Angewandte Chemie, International Edition, 51*, 12025–12028.

Gerey, B., Goure, E., Fortage, J., Pecaut, J., & Collomb, M. N. (2016). Manganese-calcium/strontium heterometallic compounds and their relevance for the oxygen-evolving center of photosystem II. *Coordination Chemistry Reviews, 319*, 1–24.

Grabolle, M., Haumann, M., Müller, C., Liebisch, P., & Dau, H. (2006). Rapid loss of structural motifs in the manganese complex of oxygenic photosynthesis by X-ray irradiation at 10-300K. *The Journal of Biological Chemistry, 281*, 4580–4588.

Guskov, A., Kern, J., Gabdulkhakov, A., Broser, M., Zouni, A., & Saenger, W. (2009). Cyanobacterial photosystem II at 2.9-Å resolution and the role of quinones, lipids, channels and chloride. *Nature Structural & Molecular Biology, 16*, 334–342.

Haumann, M., Liebisch, P., Muller, C., Barra, M., Grabolle, M., & Dau, H. (2005). Photosynthetic O_2 formation tracked by time-resolved x-ray experiments. *Science, 310*, 1019–1021.

Hellmich, J., Bommer, M., Burkhardt, A., Ibrahim, M., Kern, J., Meents, A., Müh, F., Dobbek, H., & Zouni, A. (2014). Native-like photosystem II superstructure at 2.44Å resolution through detergent extraction from the protein crystal. *Structure, 22*, 1607–1615.

Holzwarth, A. R., Müller, M. G., Reus, M., Nowaczyk, M., Sander, J., & Rögner, M. (2006). Kinetics and mechanism of electron transfer in intact photosystem II and in the isolated reaction center: Pheophytin is the primary electron acceptor. *Proceedings of the National Academy of Sciences of the United States of America, 103*, 6895–6890.

Ishikita, H. (2019). Protein environment that facilitates proton transfer and electron transfer in photosystem II. In J. Barber, A. V. Ruban, & P. J. Nixon (Eds.), *Oxygen production and reduction in artificial and natural systems* (pp. 191–208). Singapore: World Scientific Publishing Co. Pte Ltd.

Isobe, H., Shoji, M., Yamanaka, S., Umena, Y., Kawakami, K., Kamiya, N., Shen, J. R., & Yamaguchi, K. (2012). Theoretical illumination of water-inserted structures of the $CaMn_4O_5$-cluster in the S_2 and S_3 states of oxygen-evolving complex of photosystem II: Full geometry optimizations by B3LYP hybrid density functional. *Dalton Transactions, 41*, 13727–13740.

Junge, W. (2019). Oxygenic photosynthesis: History, status and perspective. *Quarterly Reviews of Biophysics, 52*, e1.

Kamiya, N., & Shen, J. R. (2003). Crystal structure of oxygen-evolving photosystem II from *Thermosynechococcus vulcanus* at 3.7 Å resolution. *Proceedings of the National Academy of Sciences of the United States of America, 100*, 98–103.

Kanady, J. S., Tsui, E. Y., Day, M. W., & Agapie, T. (2011). A synthetic model of the Mn_3Ca subsite of the oxygen-evolving complex in photosystem II. *Science, 333*, 733–736.

Kanady, J. S., Lin, P. H., Carsch, K. M., Nielsen, R. J., Takase, M. K., Goddard, W. A., & Agapie, T. (2014). Toward models for the full oxygen-evolving complex of photosystem II by ligand coordination to lower the symmetry of the Mn_3CaO_4 cubane: Demonstration that electronic effects facilitate binding of a fifth metal. *Journal of the American Chemical Society, 136*, 14373–14376.

Kärkäs, M. D., Verho, O., Johnston, E. V., & Åkermark, B. (2014). Artificial photosynthesis: Molecular systems for catalytic water oxidation. *Chemical Reviews, 114*, 11863–12001.

Kawashima, K., Takaoka, T., Kimura, H., Saito, K., & Ishikita, H. (2018). O_2 evolution and recovery of the water-oxidizing enzyme. *Nature Communications, 9*, 1247.

Kern, J., Chatterjee, R., Young, I. D., Fuller, F. D., Lassalle, L., Ibrahim, M., Gul, S., Fransson, T., Brewster, A. S., Alonso-Mori, R., et al. (2018). Structures of the intermediates of Kok's photosynthetic water oxidation clock. *Nature, 563*, 421–425.

Kok, B., Forbush, B., & McGloin, M. (1970). Cooperation of charges in photosynthetic O_2 evolution. I. A linear four step mechanism. *Photochemistry and Photobiology, 11*, 457–475.

Koua, F. H. M., Umena, Y., Kawakami, K., & Shen, J. R. (2013). Structure of Sr-substituted photosystem II at 2.1 Å resolution and its implications in the mechanism of water oxidation. *Proceedings of the National Academy of Sciences of the United States of America, 110*, 3889–3894.

Krewald, V., Retegan, M., Cox, N., Messinger, J., Lubitz, W., DeBeer, S., Neese, F., & Pantazis, D. A. (2015). Metal oxidation states in biological water splitting. *Chemical Science, 6*, 1676–1695.

Krewald, V., Retegan, M., Neese, F., Lubitz, W., Pantazis, D. A., & Cox, N. (2016). Spin state as a marker for the structural evolution of nature's water splitting catalyst. *Inorganic Chemistry, 55*, 488–501.

Limburg, J., Vrettos, J. S., Liable-Sands, L. M., Rheingold, A. L., Crabtree, R. H., & Brudvig, G. W. (1999). A functional model for O-O bond formation by the O_2-evolving complex in photosystem II. *Science, 283*, 1524–1527.

Liu, W., & Thorp, H. H. (1993). Bond valence sum analysis of metal-ligand bond lengths in metalloenzymes and model complexes. 2. Refined distances and other enzymes. *Inorganic Chemistry, 32*, 4102–4105.

Lubitz, W., Chrysina, M., & Cox, N. (2019). Water oxidation in photosystem II. *Photosynthesis Research, 142*, 105–125.

McEvoy, J. P., & Brudvig, G. W. (2006). Water-splitting chemistry of photosystem II. *Chemical Reviews, 106*, 4455–4483.

Mukherjee, S., Stull, J. A., Yano, J., Stamatatos, T. C., Pringouri, K., Stich, T. A., Abboud, K. A., Britt, R. D., Yachandra, V. K., & Christou, G. (2012). Synthetic model of the asymmetric $[Mn_3CaO_4]$ cubane core of the oxygen-evolving complex of photosystem II. *Proceedings of the National Academy of Sciences of the United States of America, 109*, 2257–2262.

Mukhopadhyay, S., Mandal, S. K., Bhaduri, S., & Armstrong, W. H. (2004). Manganese clusters with relevance to photosystem II. *Chemical Reviews, 104*, 3981–4026.

Mullins, C. S., & Pecoraro, V. L. (2008). Reflections on small molecule manganese models that seek to mimic photosynthetic water oxidation chemistry. *Coordination Chemistry Reviews, 252*, 416–443.

Najafpour, M. M., Renger, G., Hołyńska, M., Moghaddam, A. N., Aro, E. M., Carpentier, R., Nishihara, H., Eaton-Rye, J. J., Shen, J. R., & Allakhverdiev, S. I. (2016). Manganese compounds as water-oxidizing catalysts: From the natural water-oxidizing complex to nanosized manganese oxide structures. *Chemical Reviews, 116*, 2886–2936.

Nelson, N., & Yocum, C. F. (2006). Structure and function of photosystem I and II. *Annual Review of Plant Biology, 57*, 521–565.

Pantazis, D. A. (2018). Missing pieces in the puzzle of biological water oxidation. *ACS Catalysis, 8*, 9477–9507.

Pantazis, D. A., Ames, W., Cox, N., Lubitz, W., & Neese, F. (2012). Two interconvertible structures that explain the spectroscopic properties of the oxygen-evolving complex of photosystem II in the S_2 state. *Angewandte Chemie, International Edition, 51*, 9935–9940.

Paul, S., Neese, F., & Pantazis, D. A. (2017). Structural models of the biological oxygen-evolving complex: Achievements, insights, and challenges for biomimicry. *Green Chemistry, 19*, 2309–2325.

Pauling, L. (1929). The principles determining the structure of complex ionic crystals. *Journal of the American Chemical Society, 51*, 1010–1026.

Peloquin, J. M., & Britt, R. D. (2001). EPR/ENDOR characterization of the physical and electronic structure of the OEC Mn-cluster. *Biochimica et Biophysica Acta, 1503*, 96–111.

Peloquin, J. M., Campbell, K. A., Randall, D. W., Evanchik, M. A., Pecoraro, V. L., Armstrong, W. H., & Britt, R. D. (2000). ^{55}Mn ENDOR of the S_2-state multiline EPR signal of photosystem II: Implications on the structure of the tetranuclear Mn cluster. *Journal of the American Chemical Society, 122*, 10926–10942.

Perez-Navarro, M., Neese, F., Lubitz, W., Pantazis, D. A., & Cox, N. (2016). Recent developments in biological water oxidation. *Current Opinion in Chemical Biology, 31*, 113–119.

Petrouleas, V., & Crofts, A. R. (2005). The iron-quinone acceptor complex. In T. J. Wydrzynski & K. Satoh (Eds.), *Photosystem II: The light-driven water: Plastoquinone oxidoreductase* (pp. 177–206). Springer: Dordrecht.

Renger, G. (2012). Mechanism of light induced water splitting in photosystem II of oxygen evolving photosynthetic organisms. *Biochimica et Biophysica Acta, 1817*, 1164–1176.

Ruettinger, W. F., Campana, C., & Dismukes, G. C. (1997). Synthesis and characterization of $Mn_4O_4L_6$ complexes with cubane-like core structure: A new class of models of the active site of the photosynthetic water oxidase. *Journal of the American Chemical Society, 119*, 6670–6671.

Saito, K., Rutherford, A. W., & Ishikita, H. (2013). Mechanism of proton-coupled quinone reduction in photosystem II. *Proceedings of the National Academy of Sciences of the United States of America, 110*, 954–959.

Satoh, K., Wydrzynski, T. J., & Govindjee. (2005). Introduction to photosystem II. In T. J. Wydrzynski & K. Satoh (Eds.), *Photosystem II: The light-driven water: Plastoquinone oxidoreductase* (pp. 11–22). Springer: Dordrecht.

Sauer, K., Yano, J., & Yachandra, V. K. (2008). X-ray spectroscopy of the photosynthetic oxygen-evolving complex. *Coordination Chemistry Reviews, 252*, 318–335.

Shen, J. R. (2015). The structure of photosystem II and the mechanism of water oxidation in photosynthesis. *Annual Review of Plant Biology, 66*, 23–48.

Siegbahn, P. E. M. (2009). Structures and energetics for O_2 formation in photosystem II. *Accounts of Chemical Research, 42*, 1871–1880.

Siegbahn, P. E. M. (2013). Water oxidation mechanism in photosystem II, including oxidations, proton release pathways, O-O bond formation and O_2 release. *Biochimica et Biophysica Acta, 1827*, 1003–1019.

Siegbahn, P. E. M. (2017). Nucleophilic water attack is not a possible mechanism for O-O bond formation in photosystem II. *Proceedings of the National Academy of Sciences of the United States of America, 114*, 4966–4968.

Styring, S., Sjöholm, J., & Mamedov, F. (2012). Two tyrosines that changed the world: Interfacing the oxidizing power of photochemistry to water splitting in photosystem II. *Biochimica et Biophysica Acta, 1817*, 76–87.

Su, X., Ma, J., Wei, X., Cao, P., Zhu, D., Chang, W., Liu, Z., Zhang, X., & Li, M. (2017). Structure and assembly mechanism of plant $C_2S_2M_2$-type PSII-LHCII supercomplex. *Science, 357*, 815–820.

Suga, M., Akita, F., Hirata, K., Ueno, G., Murakami, H., Nakajima, Y., Shimizu, T., Yamashita, K., Yamamoto, M., Ago, H., et al. (2015). Native structure of photosystem II at 1.95Å resolution revealed by a femtosecond X-ray laser. *Nature, 517*, 99–103.

Suga, M., Akita, F., Sugahara, M., Kubo, M., Nakajima, Y., Nakane, T., Yamashita, K., Umena, Y., Nakabayashi, M., Yamane, T., et al. (2017). Light-induced structural changes and the site of O=O bond formation in PSII caught by XFEL. *Nature, 543*, 131–135.

Suga, M., Akita, F., Yamashita, K., Nakajima, Y., Ueno, G., Li, H., Yamane, T., Hirata, K., Umena, Y., Yonekura, S., et al. (2019). An oxyl/oxo mechanism for oxygen-oxygen coupling in PSII revealed by an x-ray free-electron laser. *Science, 366*, 334–338.

Tanaka, A., Fukushima, Y., & Kamiya, N. (2017). Two different structures of the oxygen-evolving complex in the same polypeptide frameworks of photosystem II. *Journal of the American Chemical Society, 139*, 1718–1721.

Tommos, C., & Babcock, G. T. (1998). Oxygen production in nature: A light-driven metalloradical enzyme process. *Accounts of Chemical Research, 31*, 18–25.

Tsui, E. Y., & Agapie, T. (2013). Reduction potentials of heterometallic manganese–oxido cubane complexes modulated by redox-inactive metals. *Proceedings of the National Academy of Sciences of the United States of America, 110*, 10084–10088.

Tsui, E. Y., Kanady, J. S., & Agapie, T. (2013). Synthetic cluster models of biological and heterogeneous manganese catalysts for O_2 evolution. *Inorganic Chemistry, 52*, 13833–13848.

Umena, Y., Kawakami, K., Shen, J. R., & Kamiya, N. (2011). Crystal structure of oxygen-evolving photosystem II at a resolution of 1.9Å. *Nature, 473*, 55–60.

van Gorkom, H. J., & Yocum, C. F. (2005). The calcium and chloride cofactor. In T. J. Wydrzynski & K. Satoh (Eds.), *Photosystem II: The light-driven water: Plastoquinone oxidoreductase* (pp. 307–328). Springer: Dordrecht.

Vass, I., & Styring, S. (1991). pH-dependent charge equilibria between tyrosine-D and the S states in photosystem II. Estimation of relative midpoint redox potentials. *Biochemistry, 30*, 830–839.

Vinyard, D. J., Khan, S., & Brudvig, G. W. (2015). Photosynthetic water oxidation: Binding and activation of substrate water for O-O bond formation. *Faraday Discussions, 185*, 37–50.

Vrettos, J. S., Limburg, J., & Brudvig, G. W. (2001). Mechanism of photosynthetic water oxidation: Combining biophysical studies of photosystem II with inorganic model chemistry. *Biochimica et Biophysica Acta, 1503*, 229–245.

Wei, X., Su, X., Cao, P., Liu, X., Chang, W., Li, M., Zhang, X., & Liu, Z. (2016). Structure of spinach photosystem II–LHCII supercomplex at 3.2Å resolution. *Nature, 534*, 69–74.

Yamaguchi, K., Shoji, M., Isobe, H., Yamanaka, S., Kawakami, T., Yamada, S., Katouda, M., & Nakajima, T. (2018). Theory of chemical bonds in metalloenzymes XXI. Possible mechanisms of water oxidation in oxygen evolving complex of photosystem II. *Molecular Physics, 116*, 717–745.

Yano, J., & Yachandra, V. (2014). Mn_4Ca-cluster in photosynthesis: Where and how water is oxidized to dioxygen. *Chemical Reviews, 114*, 4175–4205.

Yano, J., Kern, J., Irrgang, K. D., Latimer, M. J., Bergmann, U., Glatzel, P., Pushkar, Y., Biesiadka, J., Loll, B., Sauer, K., et al. (2005). X-ray damage to the Mn_4Ca complex in single crystals of photosystem II: A case study for metalloprotein crystallography. *Proceedings of the National Academy of Sciences of the United States of America, 102*, 12047–12052.

Yano, J., Kern, J., Sauer, K., Latimer, M. J., Pushkar, Y., Biesiadka, J., Loll, B., Saenger, W., Messinger, J., Zouni, A., et al. (2006). Where water is oxidized to dioxygen: Structure of the photosynthetic Mn_4Ca cluster. *Science, 314*, 821–825.

Yocum, C. F. (2008). The calcium and chloride requirements of the O_2 evolving complex. *Coordination Chemistry Reviews, 252*, 296–305.

Young, I. D., Ibrahim, M., Chatterjee, R., Gul, S., Fuller, F. D., Koroidov, S., Brewster, A. S., Tran, R., Alonso-Mori, R., Kroll, T., et al. (2016). Structure of photosystem II and substrate binding at room temperature. *Nature, 540*, 453–457.

Zhang, C. (2007). Low-barrier hydrogen bond plays key role in active photosystem II – A new model for photosynthetic water oxidation. *Biochimica et Biophysica Acta, 1767*, 493–499.

Zhang, C. (2015). The first artificial Mn_4Ca-cluster mimicking the oxygen-evolving center in photosystem II. *Science China. Life Sciences, 58*, 816–817.

Zhang, C. (2016). From natural photosynthesis to artificial photosynthesis. *Scientia Sinica Chimica, 46*, 1101–1109.

Zhang, C., & Kuang, T. (2018). A new milestone for photosynthesis. *National Science Review, 5*, 444–445.

Zhang, C., Pan, J., Li, L., & Kuang, T. (1999). New structure model of oxygen-evolving center and mechanism for oxygen evolution in photosynthesis. *Chinese Science Bulletin, 44*, 2209–2215.

Zhang, C., Chen, C., Dong, H., Shen, J. R., Dau, H., & Zhao, J. (2015). A synthetic Mn_4Ca-cluster mimicking the oxygen-evolving center of photosynthesis. *Science, 348*, 690–693.

Zhang, M., Bommer, M., Chatterjee, R., Hussein, R., Yano, J., Dau, H., Kern, J., Dobbek, H., & Zouni, A. (2017). Structural insights into the light-driven auto-assembly process of the water-oxidizing Mn_4CaO_5-cluster in photosystem II. *eLife, 6*, e26933.

Zouni, A., Witt, H. T., Kern, J., Fromme, P., Kraub, N., Saenger, W., & Orth, P. (2001). Crystal structure of photosystem II from synechococcus elongatus at 3.8 Å resolution. *Nature, 409*, 739–743.